IRIS2 : a working infrared multi-object spectrograph & camera.

C.G. Tinney, S.D. Ryder, S.C. Ellis, V. Churilov, J. Dawson, G. Smith, L. Waller, J. Whittard, R.Haynes, A.Lankshear, J.R.Barton, C.J.Evans, K.Shortridge, T.Farrell, J.Bailey

Anglo-Australian Observatory, PO Box 296, Epping NSW 1710, Australia

ABSTRACT

IRIS2 is a near-infrared imager and spectrograph based on a HAWAII1 HgCdTe detector. It provides wide-field (7.7'×7.7') imaging capabilities at 0.4486"/pixel sampling, long-slit spectroscopy at $\lambda/\Delta\lambda\approx2400$ in each of the J, H and K passbands, and the ability to do multi-object spectroscopy in up to three masks. These multi-slit masks are laser cut, and have been manufactured for both traditional multiple slit work (≈20-40 objects in a 3'×7.4' field-of-view), multiple slit work in narrow-band filters (≈100 objects in a 5'×7.4' field-of-view), and micro-hole spectroscopy in narrow-band filters allowing the observation of ≈200 objects in a 5'×7.4' field.

Keywords: infrared: general - instrumentation: spectrographs - techniques: image processing

1.INTRODUCTION

The IRIS2[1] instrument is a near-infrared (λ= 0.9-2.5 μm) imager and spectrograph designed and manufactured by the Anglo-Australian Observatory (AAO) for use on the 3.9m Anglo Australian Telescope (AAT). It is an all-refracting nine element focal-reducing collimator-camera[2], which is installed at the AAT's Cassegrain focus. Primarily used in an *f*/8 beam, it can also (with a telescope top-end change) be used in the *f*/15 & *f*/36 beams. At *f*/8 it provides a final *f*-ratio at its HAWAII HgCdTe detector of *f*/2.2, or a plate scale of 0.4486/"pixel, resulting in a field-of-view of 7.7' on a side. IRIS2 contains just 5 mechanisms[3,4]. In order from the entrance window to the detector, they are:

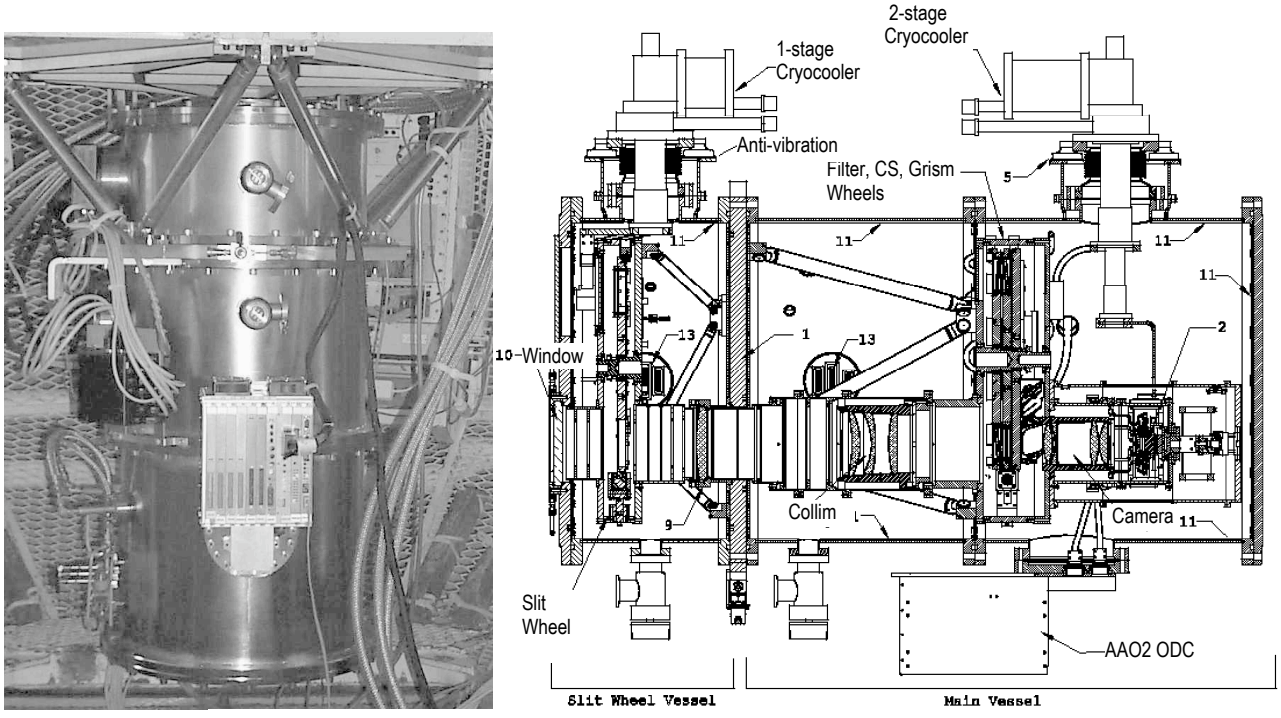

Figure 1 - IRIS2 at the AAT Cassegrain focus (left) and layout (right)

- a **slit** wheel (in the fore-dewar), containing two 1" long slits, an open position (for imaging), three multi-slit mask positions, an opaque "dark" position, and a matrix mask with 75μm holes on a 3mm grid;
- a **filter** wheel containing MKO J,H,K,Ks filters, methane filters and a range of narrow band filters
- a **cold stop** wheel at the 50mm diameter pupil, also containing additional narrow band and short wavelength filters which can be used without a cold stop;
- a **grism** wheel containing two sapphire grisms (replica transmission gratings bonded to sapphire prisms), a pupil imager for optical alignment of the instrument with the telescope, and a dark position; and,
- a detector **focus** mechanism, which adjusts the spacing between the detector and the optical train.

The IRIS2 filters were acquired as part of one of the "Mauna Kea Observatories" infrared filter consortia. J,H,K and Ks filters were acquired from OCLI of Santa Rosa, CA in 1998, and a set of narrow- and intermediate-band filters were acquired from NDC Infrared Engineering, Essex, UK between 2000 and 2002. The J,H,K,Ks filters were manufactured to the ``Mauna Kea Observatories Near-Infrared Filter Set'' specifications[5]. The narrow- and intermediate-band set are as specified by A.Tokunaga[6].

IRIS2's grisms are innovative, in that they were manufactured using sapphire as the prism component. Sapphire's higher refractive index (compared to typical infrared prism materials) delivers a larger angular deviation into the replica grating on the grism, delivering moderate dispersions with reasonable throughput[*]. For a 1" (150μm) slit at the entrance of IRIS2, this results in a 2-pixel spectral resolution of $\lambda/\Delta\lambda$=2400.

All of IRIS2's components are contained in a dual vacuum vessel : the "fore-dewar" containing a the slit wheel, and the "main dewar" containing all the other components (optics, filter, grism and coldstop wheels, and the detector). Both dewars are refrigerated using their own closed-cycle coolers. This dual dewar design allows the main dewar to be kept permanently cold (even when not mounted on the telescope), since only the much smaller fore-dewar must be opened to exchange multislit masks in the slit wheel. Since commissioning the IRIS2 main dewar has been cycled less than once a year, protecting the sensitive detector, as well as optical and mechanical in the main dewar.

2.OPTICAL AND MECHANICAL PERFORMANCE

The matrix mask installed in the slit wheel has been a critical component in the evaluation of the imaging and mechanical performance of IRIS2. This was drilled with 75μm holes (equivalent to 1.114 pixels) on a 3mm grid. While manufacturing tolerances meant that there is some variation in the diameters of these mask holes, the mask nonetheless permits precise evaluation across the whole field of IRIS2's image quality, camera focus, focus variation, flexure, detector and focal plane alignment, and astrometric distortion.

There is some curvature of the IRIS2 focal plane at the detector, but this is sufficiently small that a best focus can be achieved delivering images of <1.2 pixels full-width at half maximum (FWHM) over the whole field. Given the mask itself delivers 1-1.1 pixel (FWHM) images, the image quality of the IRIS2 optical train is better than 0.3 arcseconds over the whole field (see Figure 2).

IRIS2 (like all focal reducers) introduces astrometric distortion. The plate scale in the corners of the detector is ≈1% smaller than that at the field centre. This distortion has been measured using the IRIS2 matrix mask (Figure 3), and has been found to be entirely radial, and that it can be precisely parametrised by a polynomial

$$r = r' \, (1 - 2.4988\times10^{-6}\, r' - 4.4466\times10^{-11}\, r'^{3})$$

where r' is the radius in observed pixels from a central pixel (x_0,y_0)=(516.86,515.02), and r is the radius in pixels from (x_0,y_0) in an ideal undistorted co-ordinate system with plate scale 0.4486"/pixel. Removal of this distortion is now routinely performed by the IRIS2 data reduction system to deliver astrometrically flat reduced images to observers.

---

[*] There is a caveat. Sapphire's bi-refringence means the crystal must be aligned with the camera's optical axis. One optical supplier failed to do this, and delivered prisms which produced polarized spectra shifted by hundreds of pixels in the wavelength direction …. but lying exactly on top of each other! Luckily optical sapphire is not that expensive.

Flexure effects and mechanism reliability in IRIS2 have been examined for their scientific impact. The main scientific areas of concern are: (a) the repeatability of wheel positioning (especially for the slit wheel where repeatability directly

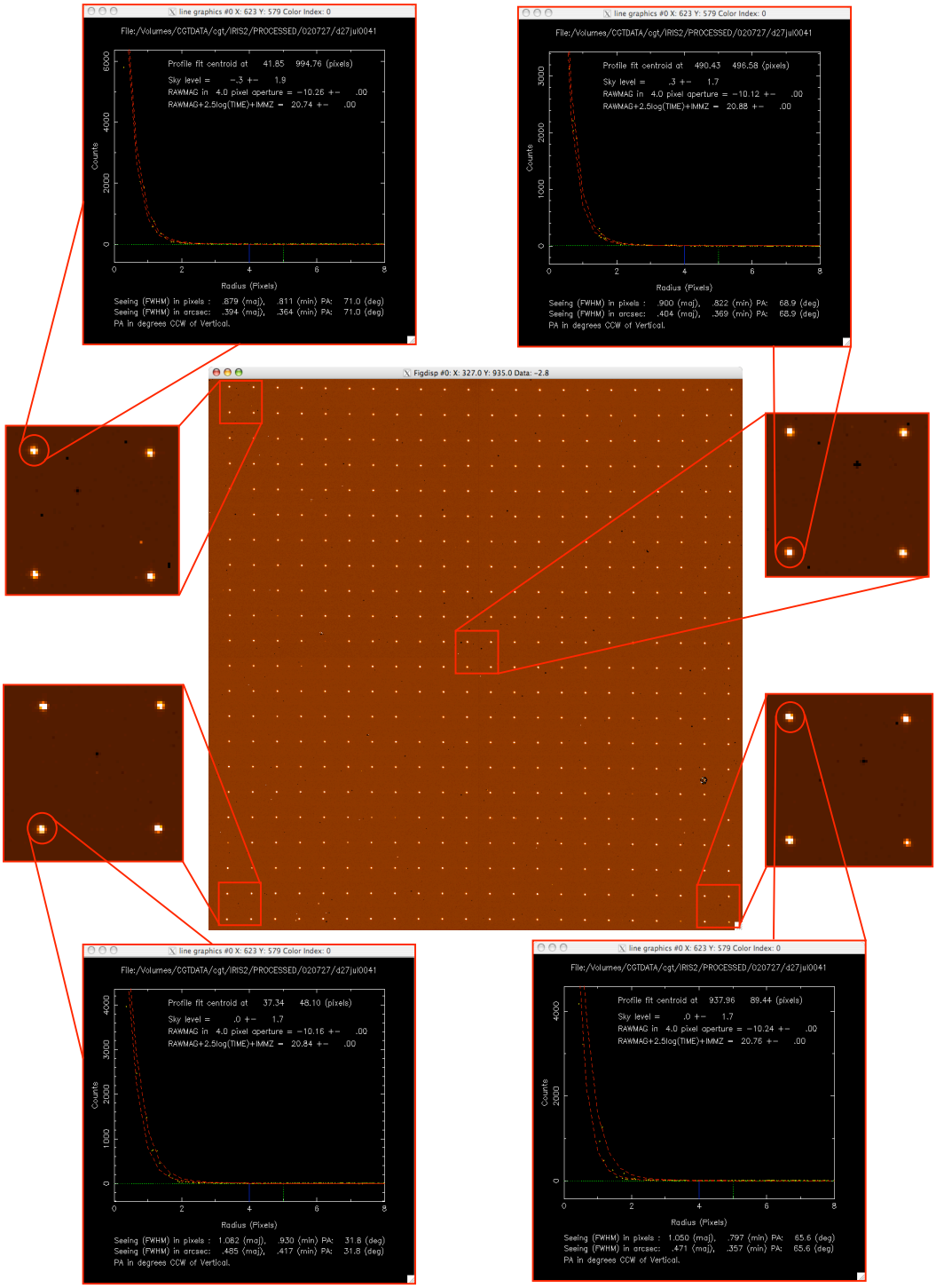

Figure 2 - IRIS2 Image Quality from matrix mask measurements

impacts the ability to do spectroscopic acquisition); (b) the stability of wheel positioning with telescope orientation (so that the slit wheel does not drift off a spectroscopic target); and (c) flexure effects on camera focus (so that the camera remains focused as the telescope moves during the night).

The repeatability of the wheel positioning has been demonstrated by wheel movement sequences at a variety of telescope orientations. At a given telescope orientation, the slit wheel has been shown to reposition to within 0.1 arcseconds (7um), so long as the wheel is always moved in the same direction (which is trivial to do for spectroscopic acquisition).

Images of the slit wheel acquired as the telescope was moved from Zenith Distance (ZD)=60° in the east, to ZD=60° in the west indicate the slit wheel shifts relative to the detector by approximately by 0.5 pixels. No perceptible flexure can be seen when the telescope is slewed in the North-South (NS) direction. Re-acquisition every ≈2h is therefore required for very long exposures (a wise practice in any case).

The camera focus has been determined to be very stable and repeatable and only needs to be re-measured, if the camera has been removed during a maintenance operation. A base focus value is then obtained for the J filter, known offsets in the camera focus are applied automatically by observing sequences for other filter and spectrographic configurations (there is a small wavelength dependence to the best focus of the optical train). Focus sequences performed with the matrix mask at a variety of telescope orientations indicate that best camera focus seems to decrease by ~35 encoder units when the telescope is moved off the vertical (in any direction) by a ZD of 41°, that is best camera focus decreases by (0.834 encoder units / degree ZD). However, the same focus sequences show that the sensitivity of image quality to defocus, is such that an offset of up to 50 encoder units has negligible impact on image quality. So flexure has no impact on the image quality of IRIS2 science data.

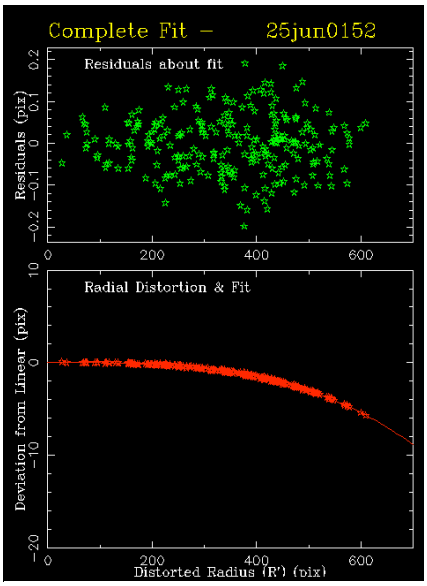

Figure 3 - IRIS2 radial astrometric distortion and fit

3.DETECTOR PERFORMANCE

IRIS2 uses a HAWAII-1 1024×1024 18.5μm pixel HgCdTe detector, driven by the AAO's new generation AAO2 Optical Detector Controllers (ODC). The AAO2 controllers (which use identical digital boards for the readout of both infrared detectors as used in IRIS2, and optical CCD detectors) use dedicated video boards specific to the HAWAII1 detector in use in IRIS2. The detector performance the combined HAWAII1 and AAO2 system delivers are summarized in Table 1 below.

The detector is used in two modes: for high background imaging observations where readout speed is critical, a Double Read Mode (DRM) is employed. The array is reset; a read is done, followed by a second read at the end of the exposure. The image delivered is the difference between the two reads. There is an overhead of one array read (0.5982s) per exposure. In low-background spectroscopic applications, where exposures are longer and read noise is critical, Multiple Read Mode (MRM) is employed. The array is reset and then non-destructively read repeatedly throughout the specified exposure time. The image delivered is a least-squares fit through the non-destructive reads. There is an overhead of one array read per exposure (which is negligible) and several seconds to complete the least-squares fit.

Inter-quadrant cross-talk[7,8], and residual image effects[9] in IRIS2 are seen at much the same level as in other HAWAII1 devices. Measured dark current performance is typically 0.1-0.2 e-/s, The cosmetic quality of the array as delivered by the AAO2 ODC is excellent (Figure 4). In both DRM and MRM modes, there are no significant structures in the images IRIS2 produces (apart from two defect regions in the HAWAII1 array, and the usual read-out register glow at

the array edges). These combined parameters give IRIS2 excellent read-noise/dark current performance for observing in low-background applications such as R=2400 spectroscopy in the J and H passbands.

Table 1 IRIS2 Detector Performance

Mode	Read Time (s)	Gain (e/adu)	Read Noise (e)	Typical Read Noise (e)	Full Well (ke-)	Non-linearity (at Full Well)
DRM	0.5982	5.3	10.0	14.1 (2 reads)	180	~1%
MRM	0.7866	4.3	8.6	4.8 (61reads)	75	~0.3%

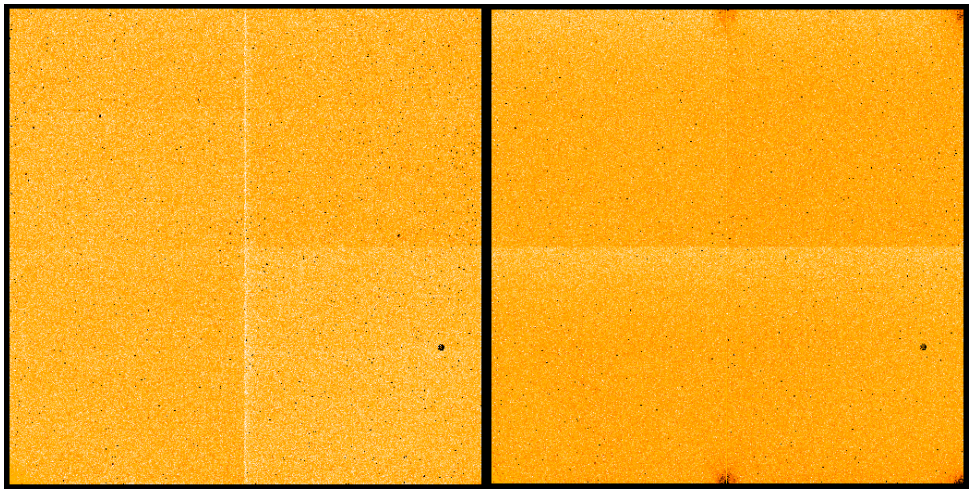

Figure 4 - IRIS2 Dark Frames. DRM 60s stretched from -10 to +20 adu (*left*) and MRM 60s, 51 reads stretched from -5 to +10 adu (*right*).

4.IRIS2 OPERATIONS

IRIS2 is operated as a distributed software system, with independent tasks running on multiple computers, which interact using the DRAMA inter-process communication system[10]. From the user's point of view operations are controlled from a single JAVA-based graphical user interface (GUI), which displays the instrument configuration, can be used to manually configure the instrument and exposure parameters, or to initiate operations from a sequence script (Figure 5). The GUI was specifically designed with a view to minimizing the number of windows and pop-ups on the screen, and for clarity of operation – only three windows are required to operate IRIS2: the main GUI, a pop-up which appears as an exposure or sequence is running, and the real-time display (RTD) which is built around ESO's SKYCAT system. Implementation of the RTD via SKYCAT has been straightforward, with the ability to add simple TCL plugins to the RTD being particularly useful, allowing the AAO to tailor interactions between users, their data, and the telescope with little effort.

Exposure sequences are constructed in TCL – a simple-minded scripting language allowing support or visiting astronomers to easily modify the "standard" sequences for specialised applications. In practice, the standard sequences see the most use for activities like: deep imaging at single positions in fixed or pseudo-random dither patterns in single or multiple filters; mapping larger areas such as 3x3 or 5x5 mosaics; making these maps for extended objects with

dithers to sky; and mapping arbitrarily large areas of sky in single or multiple filters. For spectroscopy, the most common sequences use nodding at multiple positions along the slit in one or more spectrograph configurations.

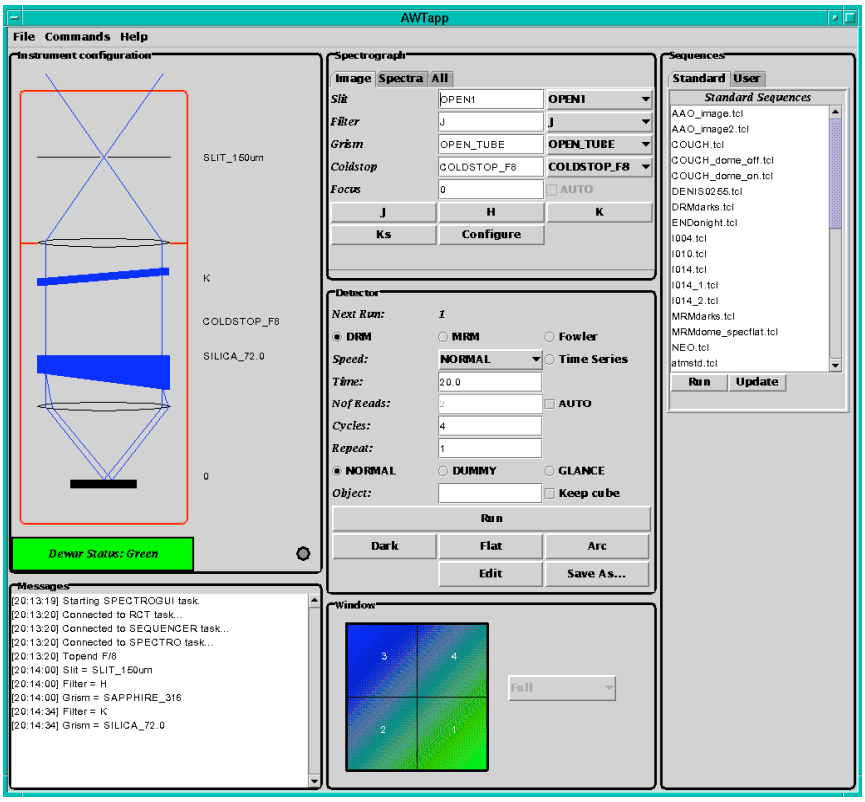

Figure 5 – The IRIS2 Java-based GUI.

These sequence scripts have been integrated with IRIS2's implementation of the ORAC-DR data reduction pipeline. ORAC-DR[11,12] is a generic data reduction pipeline originally created at the Joint Astronomy Centre, Hawaii, for use with various UKIRT and JCMT instruments. It collects sets of observations of a target in a single configuration into a *group*, and processes that group based on a set of predefined reduction *recipes*. Recipes are available for the reduction of both imaging and spectroscopic data. For example, when reducing imaging data it generates a first pass flat-field for the group by suitably normalising and medianning the data frames (if offset sky frames have been acquired, they are used). It uses these first-pass flattened data to detect objects, mask them out, and flag bad pixels. It then creates a final flat field by medianning the normalised copies of this masked data, and applies it to the raw data to create a *flattened group*. The flattened group images are re-sampled to remove astrometric disortion, objects are re-detected and offsets between images estimated using these detections. The images are then re-sampled again onto a uniform co-ordinate system to create a single *final* image. All of this processing is carried out on a dedicated data-reduction 3.3 Ghz Linux PC, resulting in fully processed images within ≈30s of an observing sequence completing – usually before the telescope has even been moved to the next observing target.

ORAC-DR recipes are straightforward to modify for specific applications – the AAO has already implemented astrometric distortion correction for IRIS2, which was not a part of the "standard" ORAC-DR distribution. Future plans include the implementation of "oversampled" and drizzling recipes. IRIS2 has quite large pixels. However, due to the nature of infrared imaging, data sets are always acquired using multiple telescope offsets. This means while an individual image may be Nyquist sampled to only 2×0.4486", the data set *as a whole* has sampling on much smaller pixel scales. This should make the derivation of final images at *at least* half the IRIS2 pixel scale possible, with a suitable processing recipe. ORAC-DR reductions of data at the telescope have been incredibly popular with astronomers. The quality of the reduction is particularly good for imaging data, and in most cases is of publication quality (Figure 5a). This allows astronomers to move immediately to analysis - rather than re-reduction - while at the telescope, or as soon as they return to their home institutions. An example of this is the large program of methane imaging being carried out at the AAT in a search for low-mass brown dwarfs ("T-dwarfs") in the 2MASS All Sky Survey[13]. The ability to immediately process reduced images in both methane filters (Figure 5b), do photometry, calibrate with 2MASS on-line data and images, and view the results, makes the identification of these T-dwarfs possible within minutes or hours of observing, allowing immediate follow-up of interesting candidates.

Figure 5 – **(a)** IRIS2 HK composite 3×3 mosaic of ρ Oph processed with ORAC-DR at the telescope - the only subsequent processing was registration and RGB conversion. The image is ≈2800 pixels, or 21', on a side. **(b)** ORAC-DR enables science at the telescope. The top three panels are IRIS2 methane (CH_4) images (*left* and *center*) and a 2MASS H-band image (*right*) of a candidate T-dwarf. 2MASS H-data calibrates the IRIS2 CH_4 colour, which is plotted vs J-H and J-K (*lower right*). Comparing with known T-dwarfs[13] we can classify this object as a T7 dwarf *at the telescope*, triggering follow-up spectroscopy. Infrared spectra[14] confirm this imaging result.

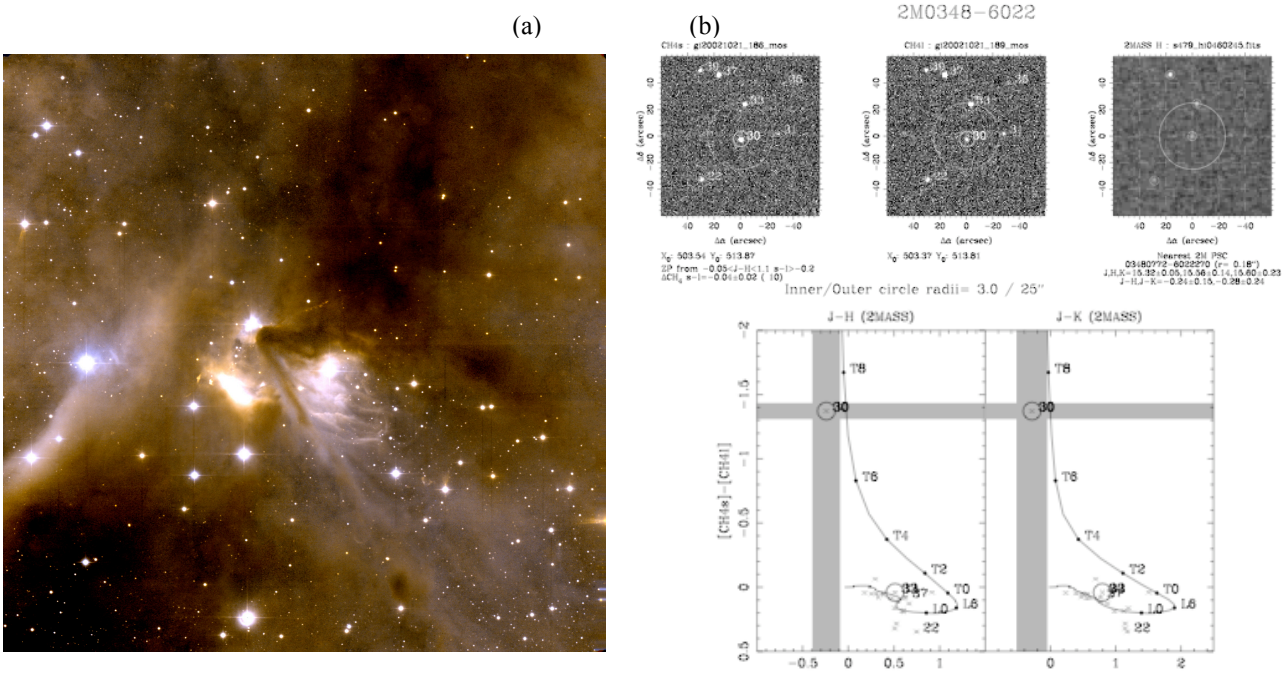

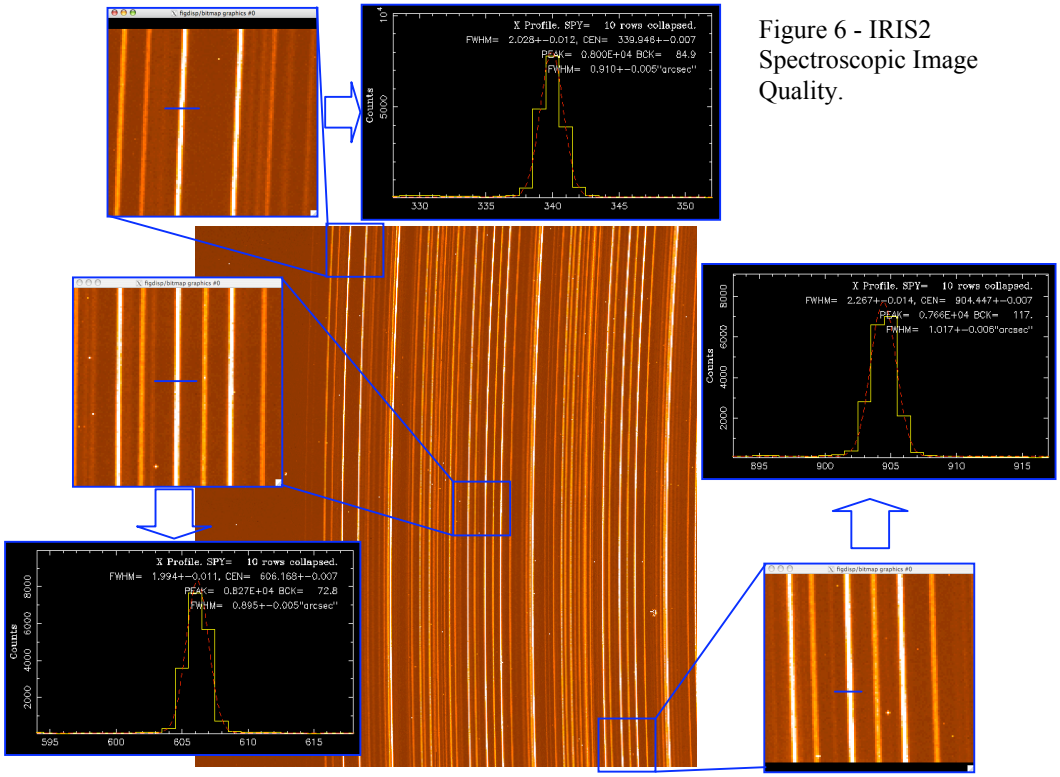

Figure 6 - IRIS2 Spectroscopic Image Quality.

5.SPECTROSCOPY

Spectra are obtained with IRIS2 using 1" slits at the telescope focal plane, and grisms and blocking filters inserted into the collimated beam. Two grisms are used to obtain 4 commonly used spectrographic configurations:

- **Js** 'Jshort' : 1.04-1.26μm at 0.23nm/pix using the Sapphire240 grism in second order with the Js filter.
- **Jl** 'Jlong' : 1.10-1.33μm at 0.23nm/pix using the Sapphire240 grism in second order with the Jl filter.
- **Hs** 'Hspect' or **H** : 1.46-1.81μm or 1.47-1.79μm at 0.34nm/pix using the Sapphire316 grism in first order with either the Hs or MKO H filters (respectively).
- **K** or **Ks** : 2.02-2.37μm or 2.02-2.31μm at 0.44nm/pix using the Sapphire240 grism in first order with either the MKO K or MKO Ks filter (respectively). The latter offers a better thermal background.

Spectroscopic image quality is generally excellent. Camera focus sequences obtained on blank sky spectra allow an optimum camera focus to be measured for each spectroscopic format, and offsets between this and the image "base focus" at J (described above) are used to set camera focus automatically. Figure 6 shows a H night sky spectral image at such a best focus, with breakouts zoomed in on regions of the image. Spectral resolutions of <2.1 pixels (FWHM for a Gaussian fit) are obtained at all wavelengths in the central regions of the detector (Y=400-600 pixels, the region usually used for single object spectroscopy), while 80% of the detector delivers resolutions of better than 2.3 pixels, and the whole detector delivers resolutions of 2.4 pixels or better.

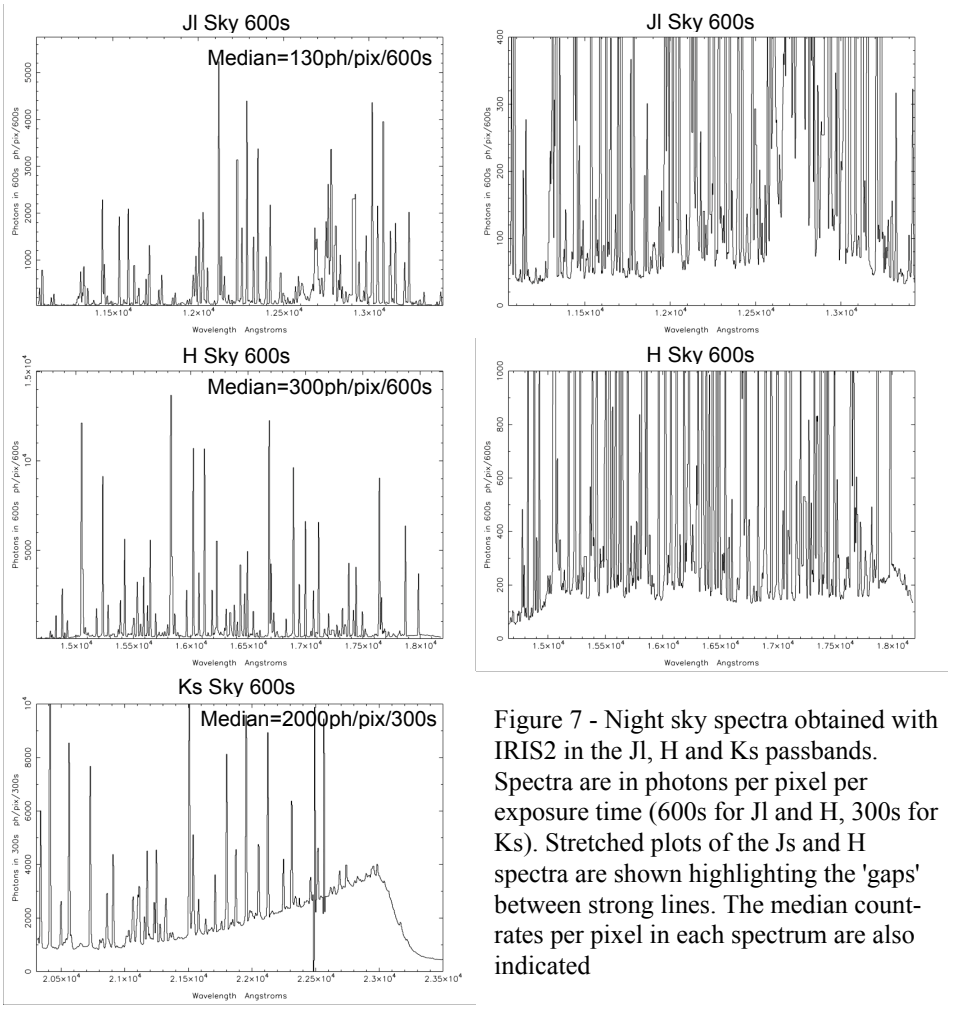

Figure 7 - Night sky spectra obtained with IRIS2 in the Jl, H and Ks passbands. Spectra are in photons per pixel per exposure time (600s for Jl and H, 300s for Ks). Stretched plots of the Js and H spectra are shown highlighting the 'gaps' between strong lines. The median count-rates per pixel in each spectrum are also indicated

Example night sky spectra obtained with the Jl, H and Ks configurations are provided in Figure 7. IRIS2 spectra provide some degree of resolution of the night sky spectrum in the J and H passbands. Weighted, binned low-resolution spectra can be obtained by binning these spectra after processing - eg. R≈400 by binning by a factor of 6. Weighting the binned result by photon-counting uncertainties means that pixels on night-sky lines receive extremely low weight in the final spectrum. Simulations indicate that the median S/N is a factor of 1.4× and 1.7× better (at J and H respectively) as a result of observing at R≈2400 followed by weighted binning to R≈400 (after sky subtraction), than would be obtained by actually observing directly in the same conditions at R≈400. Wavelength calibrations are typically obtained at the start and end of the night using a Xe arc lamp mounted on a guide probe which can be driven into the IRIS2 beam. Precise calibration during the night is obtained using the plentiful calibration spectra (ie. OH airglow emission) that nature so helpfully provides. Flat fields are obtained at the end of each night. Acquisition is

carried out using a simple interface implemented as a TCL plug-in within SKYCAT. Slit images can be fit with a polynomial parametrisation in real-time and overlaid on the IRIS2 RTD. Acquisition is then a matter of selecting a target object using IRIS2 in imaging mode with the mouse (either centroiding, or based on a RTD pixel position) and commanding the telescope to move that object onto the slit. In the final stages of faint object acquisition, these offsets are usually made by driving the guide probe head as the telescope guides, rather then driving the telescope. The slit and grism are then driven in and observing starts. Observations in J (the darkest band for IRIS2 spectroscopy) are typically background limited in 300s, which sets the timescale for nodding the telescope during an observing sequence. ORAC-DR recipes are also provided for the reduction of spectroscopic data at the telescope.

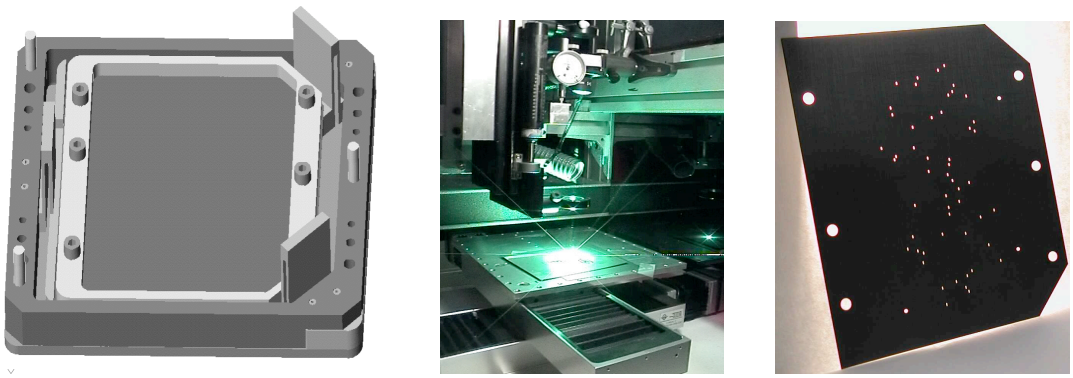

Figure 8 – Engineering realization of the IRIS2 MOS Mask holders (*left*), a mask being laser cut by Laser Micromachining Solutions (*centre*), and an IRIS2 MOS mask (*right*).

6.MULTI-OBJECT SPECTROSCOPY

The wide field-of-view and collimator-camera design of IRIS2 naturally raised the prospect of multi-object spectroscopy early in the instrument's planning phase. Unfortunately, a limited budget meant we were not able to implement the fully-fledged jukebox system, which would be necessary to interchange large numbers of masks in IRIS2. However, the choice to develop IRIS2 as a two dewar instrument, does allow the cycling of a limited set of masks in the fore-dewar. So a system for installing up to 3 Multi-Object Spectroscopy (MOS) masks in the slit wheel was implemented.

The multi-slit masks for IRIS2 are laser cut from 100μm thick, chemically-blackened brass sheet (Fig. 8). The machining is performed by Laser Micromachining Solutions, which is part of the Centre for Lasers and Applications at the Macquarie University, Sydney. The astrometric and cosmetic quality of the masks is excellent– edge roughness due to the laser cutting is tiny at ±2μm (0.013"). The major cause of edge roughness is the chemical blackening layer which can leave occlusions of size ≈10μm (0.07") at the slit edges (see Fig. 9). Differential contraction between the brass masks and the aluminium wheels could result in buckling of the masks as they are cooled to their working temperature of 100K . To prevent this, the mask is mounted in a brass frame of two parts (Fig. 8): a clamping plate; and a carrier plate. Differential thermal contraction is accommodated by incorporating three flexures between these plates. All masks are manufactured with an asymmetric set of holes around their perimeters so that they cannot be incorrectly loaded in their frames. The sky area available for cutting slits in these masks is ≈6'×7.4' – though if spectra covering 80% of the J, H or K windows are desired, this is further reduced to ≈3.5'×7.4'.

The masks are used in a temperature-controlled dewar so the moderate expansion co-efficient of brass is not an issue - only the temperature at which the masks are *cut* in the LMS workshop need be controlled to ensure adequately astrometry. The three masks can be exchanged on a timescale of days, so a maximum of three masks are offered per IRIS2 observing block (ie. per lunation).

Astrometric accuracy to one part in 3000 is required to ensure objects aren't de-centered on their slits by more than 0.2 pixels across the 600 pixel spatial range accessible to MOS. Several iterations were required to develop the scale

factor between mask manufacturing co-ordinates and arcsecond offsets on the sky – this was due to both uncertainties in the expansion coefficients of brass at these temperatures, as well as in the f/8 plate scale of the IRIS2 slit wheel (astronomers rarely need to know their instrumental plate scale to 0.03%!) As the Richey-Chretien *f*/8 focus of the AAT is astrometrically flat, the biggest challenge (once the scale factors above are known) is in getting observer's co-ordinate systems with correct astrometric coordinates on the sky. Fortunately, the availability of the astrometrically excellent 2MASS catalogue has greatly simplified this procedure.

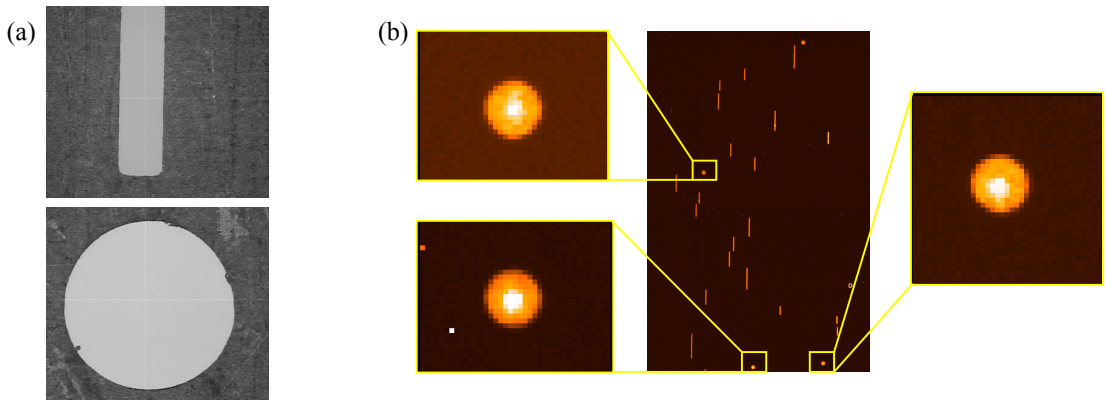

Figure 9 – (a) A 133μm wide IRIS2 MOS slit (*upper*) and 740μm diameter fiducial hole (*lower*). (b) An acquired IRIS2 MOS field in Orion showing fiducial stars in their acquisition holes (*right*).

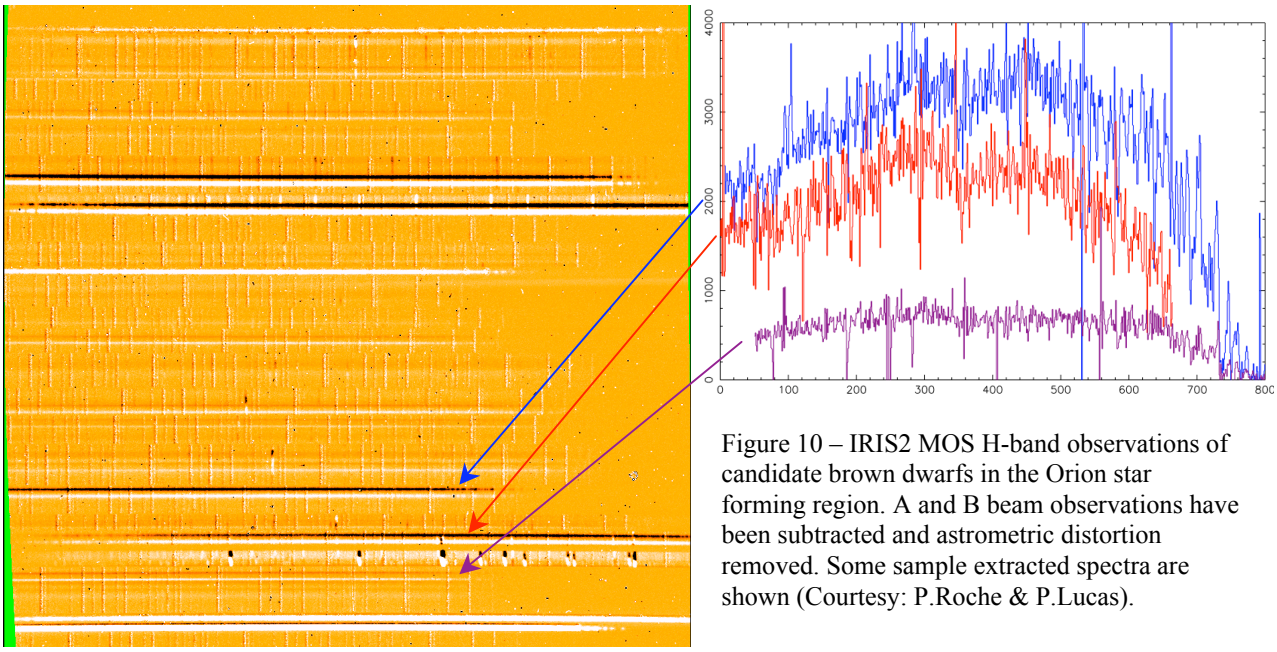

Figure 10 – IRIS2 MOS H-band observations of candidate brown dwarfs in the Orion star forming region. A and B beam observations have been subtracted and astrometric distortion removed. Some sample extracted spectra are shown (Courtesy: P.Roche & P.Lucas).

A specialised TCL plug-in within SKYCAT is used for acquisition. All masks are cut with three or four 5" holes at the positions of known fiducial stars on the same coordinate system as the target stars. Observers select these holes in an image of the MOS mask, and then take images of their target fields, and select their fiducial stars to match these holes. The TCL plug-in estimates instrument rotations (if needed) and offsets. Once the instrument rotation is close, images can be obtained *through* the 5" holes in the MOS mask for final peak-up (Fig 9).

MOS masks can be cut in essentially any orientation – masks have been cut to observe in "traditional" MOS mode (typically 10-20" long slits, along which a single object is nodded) allowing the observation of 20-40 targets per mask (see Fig. 10 for a typical example); in a multiplexed MOS mode using a narrow band filter to permit the allocation of three or four objects in 10-20" slits along the same dispersed rows (≈80-100 targets per field); and even a massively multiplexed MOS mode using pairs of 1.5" "micro-holes" separated by 10" , combined with a narrow-band filter, to allow the selection of up to 200 targets. Figure 11 below shows such a design for observations of Hα in the z=0.83 cluster MS1056-03. 211 cluster members can be allocated using pairs of 1.5" circular apertures separated by 10", with a narrow band blocking filter (Jcont), which happens to lie on Hα at the cluster redshift. These masks were manufactured for use in May 2004.

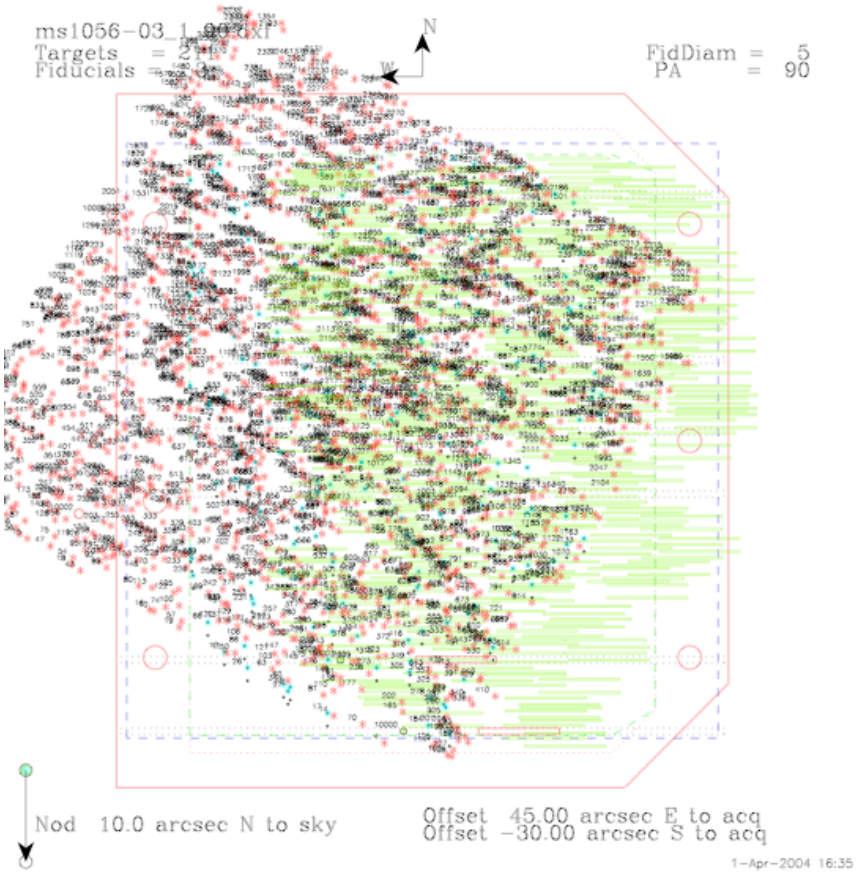

7.CONCLUSIONS

A number of design features of IRIS2 are worth highlighting. Perhaps the least sexy (but most practical) was the decision that all IRIS2 wheels would have high precision position encoding available at all wheel positions. This was done quite easily using binary-encoded optical flags. A small amount of baffling around each encoder ensures the optical flags have no impact on the detector itself, and the flags mean that when IRIS2 tries to position one of its wheels it knows *immediately* if it has been unsuccessful by even a few stepper motor steps. When this happens the wheel is able to hunt around the correct position by a few steps, and if this also fails, it automatically homes the wheel, and then repositions again – which almost always resolves the difficulty. Moreover it means that if a serious mechanical failure does arise, IRIS2 knows about it before the observer does – there is no need for staff to monitor images or spectra in a search for wheels missing steps

The provision of the matrix mask in the slit wheel of IRIS2 was of incalculable value in commissioning IRIS2 – the mask was used to check the alignment of the IRIS2 optics, examine camera focus over the whole field, measure image quality, measure astrometric distortion, measure wheel positioning accuracy, alignment of the detector with the slit

wheel, alignment of the slit wheel with the telescope axes, and on and on. We can't recommend the utility of such a mask highly enough. The ORAC-DR data reduction pipeline has been spectacularly popular with astronomers. The ability to see finally processed images, to measure exactly how faint a full data set is going, and to start scientific processing of the data at the telescope, or soon thereafter, has greatly increased IRIS2's scientific output.

The largest single "gotcha" in the IRIS2 project was the problem of dewing on the instrument's front window. IRIS2 is probably one of the first large dewars with a really cold (< 100K) interior, and a really large window (≈100mm) to be used at a damp observing site. We soon found that the typical approach to keeping dewar windows clear – flushing dry nitrogen over them – was completely inadequate. The problem was that the small radiative coupling between the window and the dewar internals, combined with the large size and low conductivity of the fused silica window, was sufficient that centre of the window was able to be lowered below 0°C. In this situation the centre of the window would ice up (rather than fog up) and no amount of dry nitrogen would stop this from happening. A variety of solutions were tried, but the only solution that worked was the installation of a second, thin silica window in front of the dewar window, to create a sealed space which could be flushed with dry nitrogen and be kept 100% free of water – in essence, double glazing the dewar. This problem should be born in mind for the coming generation of wide-field ground-based infrared instruments, most of which will have large format, low conductivity windows – even in a low humidity environment, if the centre of the dewar window drops below 0°C, every passing molecule of water will freeze out onto it!

IRIS2 was designed with wide-field science in mind, which lead to the choice of an optical design leading to quite large (0.4486") pixels. In hindsight, this has come to be seen as an inspired design decision. The size and expense of infrared detectors almost always leads to trade-offs in design between pixel sampling, and field-of-view. A point which is generally neglected in such trade-offs, is that unlike the optical where images are typically obtained as a single exposure, infrared imaging data is almost always acquired as a dithered set of multiple images. So (as pointed out in Section 4) the data set *as a whole* contains spatial information on scales much smaller than the pixel-sampling of an individual image. Given this, Nyquist-sampling the best possible seeing may *not* be the optimum design strategy for infrared imaging cameras. This is particularly true if the science goals of a camera are survey-driven, rather than being driven by the follow-up of individual objects of interest.

Acknowledgements: We wish to particular thank Dr Pat Roche for making his IRIS2 MOS data in Orion available to us in advance of publication.

REFERENCES

[1] IRIS2 WWW Page and Documentation at http://www.aao.gov.au/iris2
[2] P. Gilingham & D. Jones. "*Optical Design for IRIS2: the AAT's next Infrared Spectrometer*." In Optical and IR Telescope Instrumentation and Detectors, ed. Iye, & Moorwood, Proc. SPIE, 408, 1084-1093.
[3] V.Churilov et al. "*Engineering performance of IRIS2 infrared imaging camera and spectrograph*" In Astronomical Telescopes and Instrumentation, this proceedings. Paper 5492-105.
[4] G. Smith, V. Churilov, "*Mechanical design of the IRIS2 infrared imaging camera and spectrograph*." In Instrument Design and Performance for Optical/Infrared Ground-based Telescopes, ed. Iye, & Moorwood, Proc. SPIE Conference 4841, paper 4841-149.
[5] A.T. Tokunaga, D.A. Simons & W.D. Vacca, 2002, PASP, 114, 180
[6] http://www.ifa.hawaii.edu/~tokunaga/filterSpecs.html
[7] G.Finger & G.Nicolini, 1998. http://www.eso.org/~gfinger/hawaii_1Kx1K/crosstalk_rock/crosstalk.html
[8] C.G. Tinney, A.J. Burgasser & J.D. Kirkpatrick, 2003, AJ, 126..975T
[9] G.Finger et al. "*Megapixel Infrared Arrays at the European Southern Observatory*." Proc. SPIE, 2871, 1160-1170
[10] http://www.aao.gov.au/drama/html/dramaintro.html
[11] http://www.jach.hawaii.edu/JACpublic/UKIRT/software/oracdr/
[12] B. Cavanagh, P. Hirst, T. Jenness, F. Economou, M.J. Currie, S. Todd & S.D. Ryder, ASP Conf.Ser., 295, 237
[13] C.G. Tinney, A.J.Burgasser, J.D. Kirkpatrick & M.W. McElwain, 2004, AJ, submitted, "*Methane Imaging: A Better Way to Sniff Out T-dwarfs*"
[14] A.J.Burgasser, M.W. McElwain, J.D. Kirkpatrick, K.L. Cruz, C.G. Tinney & I.N.Reid, 2004, AJ, 127, 2856